Low mass dimuon production
in proton and ion induced interactions at the SPS

The NA38 and NA50 Collaborations

M.C. Abreu[7,a], B. Alessandro[12], C. Alexa[4], R. Arnaldi[12], J. Astruc[9], M. Atayan[14], C. Baglin[2],
A. Baldisseri[2], A. Baldit[3], M. Bedjidian[13], F. Bellaiche[13], S. Beolè[12], V. Boldea[4], P. Bordalo[7,b], A. Bussière[2],
V. Capony[2], L. Casagrande[7], J. Castor[3], T. Chambon[3], B. Chaurand[10], I. Chevrot[3], B. Cheynis[13], E. Chiavassa[12],
C. Cicalò[5], M.P. Comets[9], N. Constans[10], S. Constantinescu[4], D. Contardo[13], A. De Falco[5], G. Dellacasa[1],
N. De Marco[12], E. Descroix[13,c], A. Devaux[3], S. Dita[4], O. Drapier[13], B. Espagnon[3], J. Fargeix[3], R. Ferreira[7],
S.N. Filippov[8], F. Fleuret[10], P. Force[3], M. Gallio[12], Y.K. Gavrilov[8], C. Gerschel[9], P. Giubellino[12], M.B. Golubeva[8],
M. Gonin[10], P. Gorodetzky[11,d], A.A. Grigorian[14], J.Y. Grossiord[13], F.F. Guber[8], A. Guichard[13], J.P. Guillaud[2],
H. Gulkanyan[14], R. Hakobyan[14], R. Haroutunian[13], M. Idzik[12,e], D. Jouan[9], T.L. Karavitcheva[8], L. Kluberg[10],
R. Kossakowski[2], A.B. Kurepin[8], Y. Le Bornec[9], P. Liaud[2], C. Lourenço[6,*], M. Mac Cormick[9], P. Macciotta[5],
A. Marzari-Chiesa[12], M. Masera[12], A. Masoni[5], S. Mehrabyan[14], M. Monteno[12], S. Mourgues[3], A. Musso[12],
F. Ohlsson-Malek[13,f], P. Petiau[10], A. Piccotti[12], J.R. Pizzi[13], F. Prino[12], G. Puddu[5], C. Quintans[7], C. Racca[11],
L. Ramello[1], S. Ramos[7,b], P. Rato-Mendes[12], L. Riccati[12], A. Romana[10], B. Ronceux[2], I. Ropotar[6], P. Saturnini[3],
E. Scomparin[6,g], S. Serci[5], R. Shahoyan[7,h], S. Silva[7], M. Sitta[1], C. Soave[12], P. Sonderegger[6,b], F. Staley[2],
X. Tarrago[9], N.S. Topilskaya[8], G.L. Usai[5], J. Varela[7,b,i], E. Vercellin[12], N. Willis[9]

1 Università del Piemonte Orientale, Alessandria and INFN-Torino, Italy
2 Laboratoire de Physique des Particules (LAPP), IN2P3-CNRS, Annecy-le-Vieux, France
3 Laboratoire de Physique Corpusculaire (LPC), Université Blaise Pascal, IN2P3-CNRS, Aubière, France
4 Institute of Atomic Physics (IFA), Bucharest, Romania
5 Università di Cagliari/INFN, Cagliari, Italy
6 CERN, Geneva, Switzerland
7 Laboratório de Instrumentação e Física Experimental de Partículas (LIP), Lisbon, Portugal
8 Institute for Nuclear Research (INR), Moscow, Russia
9 Institut de Physique Nucléaire de Orsay (IPNO), Université Paris-Sud, IN2P3-CNRS, Orsay, France
10 Laboratoire de Physique Nucléaire des Hautes Energies (LPNHE), Ecole Polytechnique, IN2P3-CNRS, Palaiseau, France
11 Centre de Recherches Nucléaires, Université Louis Pasteur, IN2P3-CNRS, Strasbourg, France
12 Università di Torino/INFN, Torino, Italy
13 Institut de Physique Nucléaire de Lyon (IPNL), Université Claude Bernard, IN2P3-CNRS, Villeurbanne, France
14 Yerevan Physics Institute (YerPhI), Yerevan, Armenia

Abstract. The low mass dimuon spectra collected in p-U collisions by the NA38 experiment significantly exceeds the total cross section expected from previous analysis, done by other experiments. The 'excess' events have a harder $p_{\rm T}$ distribution than the muon pairs from η and ω Dalitz decays, expected to dominate the mass window 0.4–$0.65\,{\rm GeV}/c^2$. We conjecture that the excess events may be due to $q\bar{q}$ annihilations, negligible at low $p_{\rm T}$ but made visible by the $m_{\rm T}$ cut applied in the NA38 data. Taking this assumption to parametrise the p-U spectra, we proceed with the corresponding analysis of the S-Cu, S-U and Pb-Pb data, collected by the NA38 and NA50 experiments, comparing the measured low mass dimuon spectra with the 'expected cocktail'.

a Also at UCEH, Universidade do Algarve, Faro, Portugal
b Also at IST, Universidade Técnica de Lisboa, Lisbon, Portugal
c Now at Université Jean Monnet, Saint-Etienne, France
d Now at PCC Collège de France, Paris, France
e Now at FPNT, University of Mining and Metallurgy, Cracow, Poland
f Now at ISN, University Joseph Fourier and CNRS-IN2P3, Grenoble, France
g Now at Università di Torino/INFN, Torino, Italy
h On leave of absence from YerPhI, Yerevan, Armenia

1 Introduction

The dilepton mass spectrum in the mass region below 1.5 GeV, referred in the following as the low mass region (LMR), is expected to consist primarily of a superposition of light meson decays into lepton pairs. However, the first studies of low mass dilepton production in pp and p-A collisions, either detecting electron [1] or muon [2] pairs, observed that the number of detected lepton pairs was higher than what would be expected from the superposition of hadronic decays.

These early results are likely to be affected by the high background and by the uncertainty in the normalisation of the conventional sources (in particular, the η production cross section). Nevertheless, the indication of "anomalous low mass dilepton production" was strong enough to motivate a dedicated experiment, HELIOS/1, combining the capability to measure photons, electrons and muons. HELIOS/1 was able to show that the low mass dilepton spectra in p-Be collisions at 450 GeV can be described as a superposition of the expected contributions from light meson decays, within an uncertainty of 40–60 %, depending on the mass [3]. Besides the excellent mass resolution, the biggest advantage of this experiment was the exclusive measurement of the η Dalitz decay in $l^+l^-\gamma$, vastly improving the precision on the η normalisation.

More recently, the CERES experiment, in a joint effort with the TAPS (Two Arm Photon Spectrometer) collaboration, has also performed the measurement of the $e^+e^-\gamma$ mass distribution in p-Be and p-Au collisions, at 450 GeV. They confirmed, with improved accuracy, that the dilepton spectra produced in p-A collisions is well reproduced by the contributions from light meson decays [4,5].

The first aim of the study reported in this paper is to evaluate if the same analysis procedure is also able to provide a satisfactory description of the p-U dimuon data collected by the NA38 experiment.

While the p-A dilepton production seems to have been clarified, in the case of S-Au and Pb-Au collisions, the CERES experiment has reported [6] a rather large excess of events, particularly important in the mass region around 400–600 MeV, with respect to the expected signal, supposed to scale from the p-A yield as the number of secondary charged particles.

The HELIOS/3 experiment has reported [7] that the yield of low mass dimuons increases from p-W to S-W by more than the corresponding increase in the number of produced charged particles. HELIOS/3 has also observed that the 'excess' in dimuon production, seen in S-W collisions relative to the p-W reference data, extends through the 'intermediate mass region', up to $M \sim 2.5$ GeV.

Similar studies of that higher mass window have already been reported by the NA38 and NA50 experiments [8,9]. In the final part of the present work we will compare the low mass dimuon spectra measured in nucleus-nucleus collisions, by the NA38 (S-Cu, S-U) and NA50 (Pb-Pb)

experiments, with those 'expected sources' that we have previously identified as providing a good description of the p-U reference data. The energy of the Pb beam was 158 GeV per nucleon while the proton and sulphur beams had an energy of 200 GeV per nucleon. See [10] for previous reports of preliminary versions of this work.

2 Detector overview

The main detector element of the NA38 and NA50 experiments is the muon spectrometer, designed for the NA10 experiment and optimised for the measurement of high mass muon pairs. The angle and momentum of the muon tracks are measured in a magnetic spectrometer, with an air gap toroidal magnet placed between two sets of multi-wire proportional chambers. The dimuon trigger is provided by coincidences among four scintillator hodoscopes. The muon spectrometer is protected from the high multiplicity target region by a hadron absorber, made of ~ 5 m of graphite. It measures the muon pairs in the (lab) pseudo-rapidity interval $2.8 < \eta_{\mathrm{lab}} < 4.0$. See [11,13] for a more detailed description of the spectrometer's design and phase space coverage.

The events used in the present study were collected with segmented target systems, surrounded by a detector system that identifies the subtarget where the interaction occurred (ring scintillators in NA38; quartz blades in NA50). The number of subtargets and their exact geometrical configuration changed along the several data taking periods, keeping a thickness ~ 10–20 % of an interaction length. The space between the target box and the graphite wall was filled by a pre-absorber (made of C, BeO or Al_2O_3), to absorb as many pions and kaons as possible, before they decay to muons leading to the combinatorial background of uncorrelated (like-sign and opposite-sign) muon pairs.

The 200 GeV secondary proton beam was contaminated by ~ 30 % of pions, tagged for offline rejection by means of two threshold Cherenkov counters. See [13–15] for a more complete description of the detector components and further details on the several data taking periods relevant for this paper.

3 Data selection and background subtraction

The events used in the present study have passed the usual quality requirements imposed in the NA38/NA50 high mass studies [15]. The data analysis is performed in a restricted phase space window, in order to remove the acceptance borders of the spectrometer. To guarantee that the acceptances of the different processes, evaluated through a detailed simulation of the apparatus, are always kept higher than 1 %, the following kinematical cuts are applied: $m_T > 2 \cdot (y_{\mathrm{lab}} - 3.55)^2 + 0.9$ GeV, $3 < y_{\mathrm{lab}} < 4$ and $|\cos\theta_{\mathrm{CS}}| < 0.5$, where θ_{CS} is the angle between one muon and the beam axis in the dimuon (Collins-Soper) rest frame [12]. In the case of the Pb-Pb data, collected

---
[i] Now at CERN, Geneva, Switzerland
[*] Corresponding author: Carlos.Lourenco@cern.ch
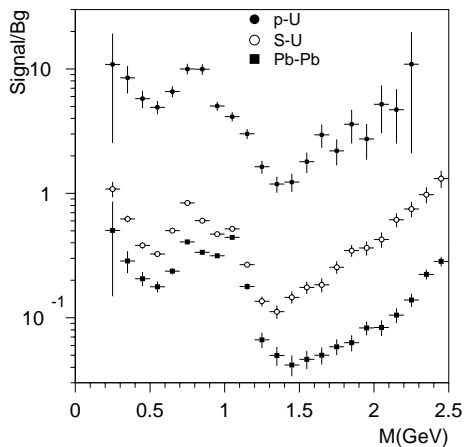
Fig. 1. Signal over background ratio as a function of the dimuon mass for p-U, S-U and Pb-Pb collisions

Table 1. Statistics available in the several data sets

	p-U	S-Cu	S-U	Pb-Pb
J/ψ	$5.0 \cdot 10^3$	$2.5 \cdot 10^3$	$14.7 \cdot 10^3$	$53.4 \cdot 10^3$
1.0–1.2 GeV	$5.5 \cdot 10^3$	$4.8 \cdot 10^3$	$35.4 \cdot 10^3$	$36.5 \cdot 10^3$

with 80 cm of Fe (instead of C) in the muon filter and with a higher magnetic field, the minimum accepted m_T value in the final analysis event sample is increased to $2 \cdot (y_{lab} - 3.55)^2 + 1.3$ GeV.

A major fraction of the collected (opposite-sign) muon pairs is due to pion and kaon decays. In view of its purely combinatorial nature, the normalisation and spectra of this contribution can be deduced from the samples of like-sign muon pairs, taken with exactly the same trigger and acceptance conditions. To ensure that the acceptances are the same, an event is selected only if it would also be accepted with any other combination of charges and of magnetic field polarity. While the high particle multiplicity of the ion collisions smears out any charge correlation at the pion or kaon production level, in the case of p-U collisions it is relatively easier to produce pairs of opposite charges. The effect of this correlation is translated into a factor R bigger than unity in the standard normalisation, $2\,R\,\sqrt{N^{++}N^{--}}$, of the estimated 'background' contribution from the measured like-sign event samples. In this study we use $R = 1.2$ for the p-U case, as suggested by a dedicated experimental study, with p-W collisions, using two setups of different hadron absorber lengths [13]. This value is in agreement with a detailed simulation study [9]. In the case of S-Cu and S-U collisions we have used $R = 1.0$.

After subtracting the estimated background contribution from the measured opposite-sign spectra, we obtain the 'signal' distributions, to be compared with the sum of the 'expected sources'. Figure 1 shows the mass dependence of the signal to background ratio in p-U, S-U and Pb-Pb collisions.

The final statistics of the several data sets used in this paper is illustrated in Table 1, by the number of signal

Table 2. Light meson production cross sections, relative to the pion cross section, at $\sqrt{s} \sim 30$ GeV

	$x\,/\,\pi^0$
η	0.053
ρ	0.065
ω	0.065
η'	0.009
ϕ	0.0033

events in the J/ψ peak and in the mass window 1.0–1.2 GeV (where the ϕ is the dominant contribution).

The normalisation of the signal mass distributions has been done using the J/ψ peak. The J/ψ cross section times branching ratio into muons, $B\sigma^\psi$, has been directly measured in the p-U, S-U and Pb-Pb event samples [15]. For S-Cu collisions we have interpolated the J/ψ cross section using the well known parametrisation $\sigma_{AB} = \sigma_0 \cdot (AB)^\alpha$, with $\alpha = 0.92$.

4 Simulation of the expected contributions

The most important sources of low mass dileptons are expected [3,4] to be the 2-body and Dalitz decays of light neutral mesons: $\eta, \rho, \omega, \phi \rightarrow \mu^+\mu^-$; $\eta, \eta' \rightarrow \mu^+\mu^-\gamma$; $\omega \rightarrow \mu^+\mu^-\pi^0$.

To attempt a complete description of the dimuon mass spectra, up to the highest masses measured by NA38/NA50, we have also simulated the contributions from J/ψ and ψ' decays, the simultaneous semileptonic decay of the D and $\bar{D}$ charmed mesons, and the quark-antiquark annihilation into muon pairs (Drell-Yan).

To describe the light meson contributions we need to know their production cross sections, their kinematical distributions (rapidity and p_T), and the way they decay into muons (branching ratios, form factors, mass distributions of the resonances).

Table 2 collects the production cross sections of the light mesons, relative to the π^0 cross section. The η, ρ and ω values, as well as the upper limit for η' production, are taken from [4]. The ϕ value was calculated from the ϕ/η ratio measured by NA27 [16]. The relative meson abundances are assumed to be independent of the collision system and energy, following the analysis done in [6].

The transverse momentum of the mesons was generated with the functional form $m_T K_1(m_T/T)$, where K_1 is the modified Bessel function and the 'inverse slope' parameter, T, is: 210 MeV in p-U; 220 MeV in S-Cu; 240 MeV in S-U and Pb-Pb. As will be shown later, this model provides a reasonable description of the measured p_T distributions.

Within a certain collision system, the same value of T is assumed for all the simulated light mesons, whose mass varies by less than a factor of 2, from m_η to m_ϕ.

The rapidity distributions were generated according to the expression $1/\cosh^2(a\,y)$, rather similar to a gaussian of $\sigma = 0.75/a$, a defining the width of the distribu-

tion. The width of the pion rapidity distribution is calculated with Landau's expression, $\sqrt{\log \gamma_{\mathrm{proj}}}$, while for the heavier mesons this value is reduced proportionally to the highest rapidity with which such mesons can be produced, $\sigma_x = \sigma_\pi\, y_{\max}(m_x)\,/\,y_{\max}(m_\pi)$. The values obtained by this procedure are in good agreement with the available measurements, e.g. $\sigma_\pi = 1.5$ and $\sigma_\psi = 0.6$, for $\sqrt{s} = 20$ GeV.

It is well known that in very asymmetric collision systems, like p-U, the peak of the pion rapidity distribution is shifted from the pp mid-rapidity value, towards the target fragmentation hemisphere. There are some indications (see, for instance, [5]) that heavier mesons experience smaller y shifts. In the present work we assume that the peak of the η rapidity distribution, in p-U collisions, is shifted by one unit, as suggested by pion distributions collected in p-A collisions [17]. The ρ and ω mesons are assumed to suffer a shift of 0.75 units, while the heavier mesons, the η' and the ϕ, are generated with a y shift of only 0.3 units. In the less asymmetric S-U collision system the corresponding values are scaled by 0.6, while for S-Cu and Pb-Pb the y distributions remain centered at mid-rapidity.

The 2-body decay of the mesons into dileptons is simulated according to a flat $\cos\theta_{\mathrm{CS}}$ distribution. The dimuon mass spectra of the ω and ϕ resonances follow the Gounaris–Sakurai parametrisation [18]. In the case of the very broad ρ resonance, a proper description of its high mass tail requires a phase space correction. In the present analysis we have followed the procedure introduced in [19], where such a correction was determined from a calculation based on the QGSM model.

The form factors of the light mesons, required to simulate the Dalitz decays, have been measured by the Lepton-G collaboration [21]. The η form factor is parametrised by the pole approximation, while the ω and η' form factors are fitted to a Breit-Wigner function. A $1 + \cos^2\theta$ angular distribution has been used for the muon pairs from Dalitz decays [20] (as done in [3]).

The absolute normalisation of the expected meson decay contributions scales with the average π^0 multiplicity times the inelastic cross section. The pion multiplicity is calculated as $0.5 \cdot \langle N_P \rangle \cdot \langle \pi^0_{NN} \rangle$, where the average number of participating nucleons, $\langle N_P \rangle$, and the nucleon-nucleon average pion multiplicity, $\langle \pi^0_{NN} \rangle$, are calculated as explained in [22]. The values obtained in this way are compared in Table 3 with the available measurements [22]. The measured and calculated multiplicities agree very well. The p-U inelastic cross section is taken from the Review of Particle Properties [23], while for the B-A nucleus-nucleus collisions we use the geometrical parametrisation $\pi\, r_0^2 \left(A^{1/3} + B^{1/3} - \beta\left(A^{-1/3} + B^{-1/3}\right)\right)^2$, with $r_0 = 1.25$ fm and $\beta = 0.83$, as proposed in [24].

The two remaining processes, open charm and Drell-Yan, were simulated with the event generator Pythia 5.7 [25], using the GRV LO 92 [26] parametrisation of the parton distribution functions, a $\langle k_T^2 \rangle$ of 1 GeV^2 and $m_c = 1.35$ GeV. The branching ratios of the charged and neutral D mesons into muons were taken from [23]. In the case of

Table 3. Multiplicities of negatively charged particles, $\langle n^- \rangle$, and of π^0s, $\langle \pi^0 \rangle$, produced in minimum bias collisions

	Measured $\langle n^- \rangle$	Calc. $\langle n^- \rangle$	Calc. $\langle \pi^0 \rangle$
pp	2.85 ± 0.03	2.85	3.34
pn	3.23 ± 0.03	3.23	3.06
nn	3.42 ± 0.13	3.42	3.34
p-Mg	$4.9\ \ \pm 0.4$	4.72	4.97
p-S	$5.0\ \ \pm 0.2$	4.99	5.25
p-Ar	5.39 ± 0.17	5.25	5.46
p-Ag	$6.2\ \ \pm 0.2$	6.45	6.70
p-Xe	6.84 ± 0.13	6.74	6.96
p-Au	$7.3\ \ \pm 0.3$	7.38	7.61
p-U	$-$	7.71	7.93
O-Cu	$29.5\ \ \pm 1.4$	26.8	26.6
O-Au	$39.4\ \ \pm 1.4$	43.0	42.3
S-S	$33.0\ \ \pm 1.9$	27.7	27.6
S-Cu	$38.6\ \ \pm 2.$	38.2	37.8
S-U	$-$	69.1	67.8
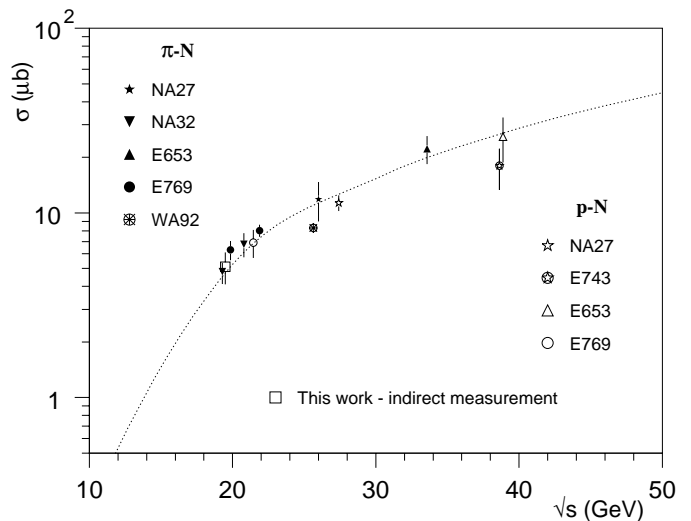
Fig. 2. Evolution of the $c\bar{c}$ cross section with $\sqrt{s}$

Drell-Yan, all the four combinations of proton and neutron interactions were generated, to take into account the influence of the valence quarks. These four generated spectra were properly weighted using the number of protons and neutrons in the projectile and target nuclei, imposing the well known linear A-dependence of Drell-Yan production. The resulting LO curves were scaled up by a K factor of 2.2, seen to provide a good description of the high mass end of the measured dimuon spectra.

In the case of the open charm process, dominated by gluon fusion, only proton-neutron collisions were generated. Assuming, as for Drell-Yan, a linear A-dependence for the open charm yield, Pythia's cross section was scaled up by the product $A \times B$, where A and B are the number of nucleons in the projectile and in the target. In this case the K factor was determined by fitting the mass region
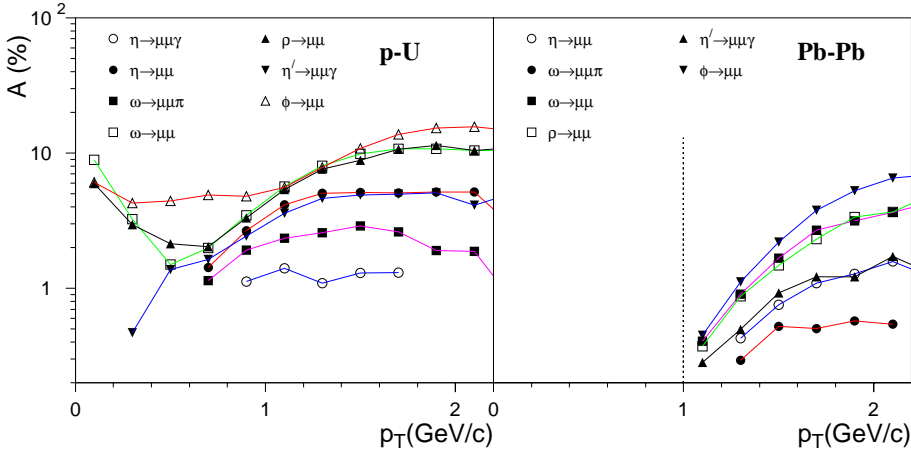
Fig. 3. Acceptance of muon pairs from the decay of light mesons, as a function of the dimuon transverse momentum, in the p-U (left) and Pb-Pb (right) setups

Table 4. Acceptances, in %, for the three different setups used to collect the data studied in this paper. The acceptance values quoted for the 'continuous' contributions, $D\bar{D}$ and Drell-Yan, correspond to the mass window 1.5–2.5 GeV

	p-U	S-Cu / S-U	Pb-Pb
$\eta \to \mu\mu$	3.8	3.9	0.9
$\rho \to \mu\mu$	4.5	4.9	1.7
$\omega \to \mu\mu$	4.5	4.9	1.7
$\phi \to \mu\mu$	5.7	5.9	1.9
$\eta \to \mu\mu\gamma$	1.2	1.0	0.1
$\omega \to \mu\mu\pi^0$	2.2	2.1	0.5
$\eta' \to \mu\mu\gamma$	3.1	3.3	0.9
$D\bar{D}$ (1.5–2.5)	13.0	13.0	3.4
DY (1.5–2.5)	16.8	16.6	6.0

below 2.5 GeV of the p-U data to a superposition of the Drell-Yan and $D\bar{D}$ contributions. The corresponding $c\bar{c}$ cross section in pp collisions, for $\sqrt{s} \sim 20$ GeV, is derived to be 5.1 ± 1.0 μb, in good agreement with the available direct measurements [27], as can be seen in Fig. 2.

All the generated events are filtered through a simulation program that reproduces the detector response, introducing all the acceptance and smearing effects. For instance, the mass resolution at the η mass is evaluated to be ~ 86 MeV (in the p-U data set). Furthermore, the simulated events have to pass the same cuts as the real data.

Table 4 presents the integrated acceptances of the several processes, in the reduced phase space defined above, for the data sets studied in this paper. The Dalitz decays of the low mass mesons are seen to be particularly affected by the high m_T cut used in the analysis of the Pb-Pb data.

Figure 3 illustrates the p_T dependence of the acceptances, in the p-U and Pb-Pb setups. We see that the NA38/NA50 detector suffers from a rather limited coverage of the low p_T region of the phase space, when looking at low mass dilepton production.

5 Analysis of the p-U data

Figure 4 shows the p-U dimuon mass spectrum together with the superposition of the several expected contributions: the hadronic decays, the muon pairs from $D\bar{D}$ decays and the Drell-Yan curve. The analysis done by HE-LIOS/1 [3] and CERES-TAPS [4] only included the light meson decays, presumably because the data of these experiments were concentrated on the mass region up to the ϕ mass. The dimuon data collected by NA38 extends up to much higher masses, where the $D\bar{D}$ and Drell-Yan processes must be included. We recall that previously reported studies [8] have already shown that the dimuon mass region above 1.5 GeV is well described by a superposition of these two processes. We stop the Drell-Yan curve at 1.5 GeV because none of the previous studies of the low mass dilepton spectra has included any DY-like contribution, since the Drell-Yan formalism is not expected to be applicable to such low mass values.

We can clearly see a difference between the measured data points and the sum of the expected sources (the 'hadronic cocktail' plus the $D\bar{D}$ decays). The data exceed the expected curve by ~ 30 % below 400 MeV and by 40 ± 3 % in the mass range 400–650 MeV. As will be shown below, the 'excess' seems to be stronger at high p_T.

We have checked that the excess cannot be attributed to decays of ρ mesons into $\pi^+\pi^-$, followed by the decays of the pions into muons. Although such a double decay would lead to muon pairs of an invariant mass around 500 MeV, the number of such events accepted in the NA38 detector is much too small, in view of the short air distance for the in-flight decay of the pions. Notice that the HELIOS/1 cocktail included such a contribution, more important in their experimental setup.

We have also verified that the excess cannot be removed by changing the rapidity shifts. For instance, reducing the rapidity shifts by a factor of two decreases the excess in the mass window below 650 MeV by only 15 % while, on the other hand, creating a 10 % default in the $\rho + \omega$ peak.

To evaluate how the p_T distributions used to generate the mesons influence the observed excess, we have redone the analysis with the functions used in [5], where a hard
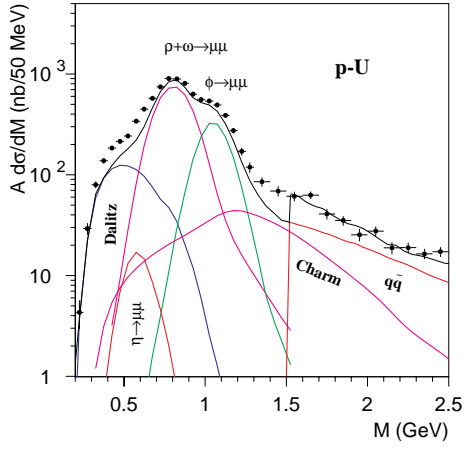
Fig. 4. Dimuon mass distribution measured in p-U collisions, compared to the superposition of expected processes
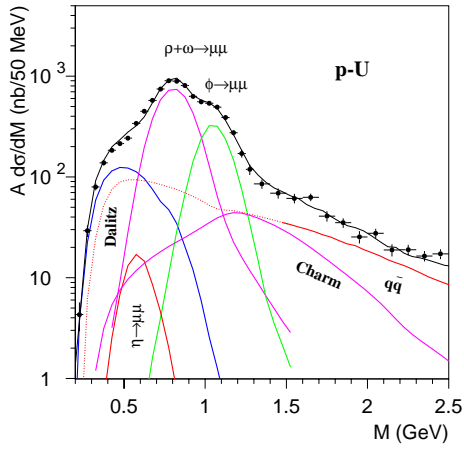
Fig. 5. Dimuon mass distribution measured in p-U collisions, compared to the new 'cocktail', including a roughly estimated contribution due to $q\bar{q}$ annihilation
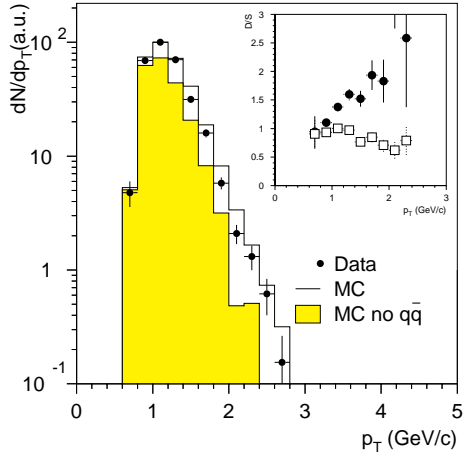
Fig. 6. Transverse momentum distributions measured in p-U, in the mass range $0.4 < M < 0.6$ GeV, compared with the expected sources. The inset shows the ratio between the data and the expected sources with (open squares) and without (filled circles) the $q\bar{q}$ annihilation process
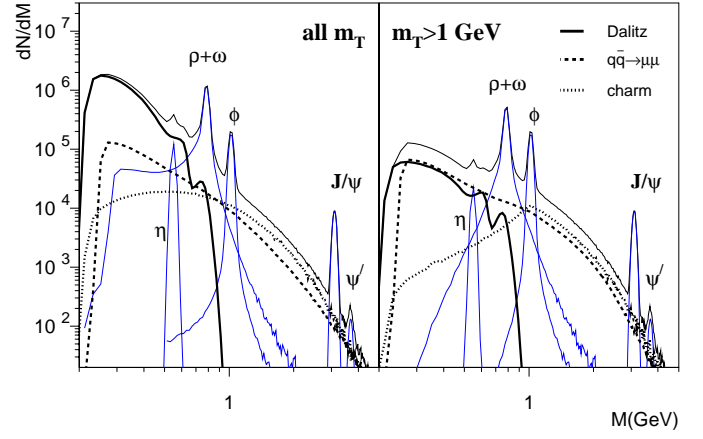
Fig. 7. Generated mass spectrum before (left) and after (right) selecting only events with m_T above 1 GeV

term

$$\alpha \times \left(1 - \frac{2\,m_T}{\sqrt{s}}\right)^c \bigg/ (1 + m_T^2)^4$$

is added to the usual $\beta\,e^{-m_T/T}$ term. For the parameters α, β and c we used the values given in [5], while for T we used 226 MeV (instead of 154 MeV), in order to retain a good description of the data (see, for instance, Fig. 9 below).

With these somewhat harder p_T distributions, the excess seen in the p-U data increases from 40 % to 50 % in the mass window 0.4–0.6 GeV and from ~ 30 % to ~ 37 % for the lower masses. This is due to the fact that most of the accepted events are in the p_T range around 1 GeV, where the relative number of generated events is reduced when we use a harder distribution.

A possible way of reproducing the data points consists in extrapolating the Drell-Yan curve down to the lowest masses. After all, there is no good reason to abruptly cut the Drell-Yan yield at 1.5 GeV. It might very well be that quark-antiquark pairs annihilate into low mass dileptons, even if such process cannot be calculated in perturbative QCD. A computation of such a process would be extremely useful but remains to be done. We made a very rough estimation of its contribution by simply extending the Drell-Yan calculation of Pythia down to the lowest Q^2 allowed by the parton distribution functions used, $Q^2_{min} = 0.25$ GeV^2.

When this $q\bar{q}$ annihilation is added to the 'expected' sources, the p-U mass distribution becomes rather well reproduced, as can be judged from Fig. 5. Furthermore, Fig. 6 shows that also the p_T distributions, for the dimuons in the mass window 0.4–0.6 GeV, become well accounted for.

Such an extrapolation to lower masses of the Drell-Yan process can be important in our kinematical window, since it is less affected by the high transverse mass cut than the rather soft muon pairs originated from Dalitz decays. This contribution should be negligible in the case of the CERES experiment, dominated by low p_T events.

Figure 7 shows that the importance of the $q\bar{q}$ annihilation process, relative to that of the Dalitz decays, strongly
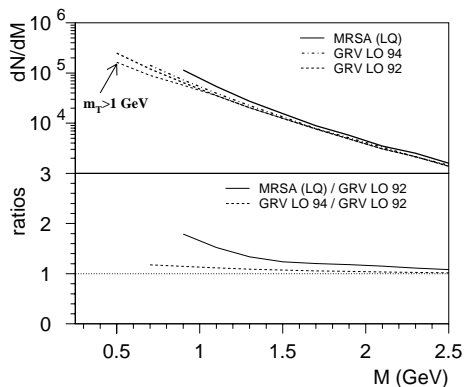
Fig. 8. Calculated mass spectrum for the $q\bar{q} \to \mu\mu$ annihilation process, for three different sets of quark distribution functions. For the GRV LO 92 set we also show the calculation for $m_T > 1$ GeV dimuons. The lower panel shows the ratios relative to the estimation done with the GRV LO 92 set, which has the lowest $Q^2_{\min}$

increases when a cut on the transverse mass is applied. These results reopen the old issue of "anomalous low mass dilepton production", in p-A collisions, now at high p_T. A complete clarification of this observation requires a high statistics experiment with a good coverage of the complete p_T spectra, at low dilepton masses. A good mass resolution and a good signal to background ratio would also be extremely helpful.

Besides motivating a future optimised experiment, these observations justify a revived effort from the theory sector. In particular, it should be possible to attempt a calculation of low mass dimuon production at high p_T. At the present moment, we are not aware of any such calculations. Our rough estimation of the $q\bar{q}$ contribution to the low mass dimuon production should only be taken as a first step towards the resolution of this anomaly and should not be considered any better than a (useful) parametrisation of the measured data. Figure 8 illustrates the big uncertainties affecting our estimation, by showing the effect of using three different sets of quark distribution functions, GRV LO 92 [26], GRV LO 94 [28] and MRS A (LQ) [29]. While the two GRV LO sets give rather close results, the MRS A (LQ) parametrisation would lead to a higher expected yield of low mass dimuons. The curves were only compared for mass values above their respective $\sqrt{Q^2_{\min}}$.

Before finishing the p-U section, we should check that the p_T distributions used in the event generation provide a reasonable description of the available data. This verification must be done using the p_T distributions of the events in the $\rho + \omega$ and ϕ peaks, where one of the contributing processes clearly dominates.

Figure 9 shows the comparison between the measured transverse momentum distributions and the sum of the expected contributions, normalised from the analysis of the dimuon mass spectra, in the $\rho + \omega$ and ϕ mass bins, where the $q\bar{q}$ annihilation process gives a negligible contribution. We can see that the measured p_T distributions

are not significantly different from what we assumed in our calculations.

6 Analysis of the ion data

In the following we will assume that the p-U dimuon data can be properly parametrised by the superposition of the sources previously described, from the J/ψ region down to the lowest measured dimuon masses, as illustrated in Fig. 5.

Using the same sources, we have calculated the dimuon mass spectra expected in the cases of S-Cu, S-U and Pb-Pb collisions. The calculation proceeds in exactly the same way as for the p-U system, scaling the hadronic cocktail with the pion multiplicity and the hard processes (open charm and Drell-Yan) with the product $A \times B$.

Figure 10 shows the dimuon mass distribution measured in S-U collisions together with the several expected contributions, including the extrapolation to low masses of the Drell-Yan mechanism. We can clearly see that the ϕ yield is substantially increased relative to the assumption that its production scales with the number of pions. A good fit of the measured ϕ peak requires increasing the ϕ cross section in S-U collisions by a factor 2.8, relative to the scaling of pion production. In what concerns the $\rho + \omega$ peak, on the contrary, the hypothesis that ω and ρ production scales as the number of pions leads to a reasonable description of the data (the best fit would require a yield enhanced by only $\sim 20\%$).

We can also appreciate from Fig. 10 the magnitude and extension of the 'excess' affecting the intermediate mass continuum. As previously reported in [8,9], an enhancement of open charm production provides a possible explanation of this observation. However, we can easily see that such a change would have no visible effect on the mass region below ~ 1.2 GeV.

The corresponding comparison between data and expected processes in the case of Pb-Pb collisions is presented in Fig. 11. There is a strong enhancement in the ϕ and higher mass regions. The apparent agreement seen in the low mass region, however, should be taken with care, since this data set suffers from the particularly strong m_T cut applied by the detector when optimised for J/ψ studies.

Figure 12 compares the dimuon mass spectra measured in S-Cu and S-U collisions with the sum of the corresponding expected sources. Notice that these data sets were collected in the same data taking period, with exactly the same apparatus, apart from the change of target. Unfortunately, the data sample collected with the Cu target has much less statistics, as compared to the S-U data set (see Table 1). Besides, the background subtraction procedure is more uncertain, since the exact value of R is not so well known for the lighter collision systems. These problems should not significantly affect the mass window of the resonances.
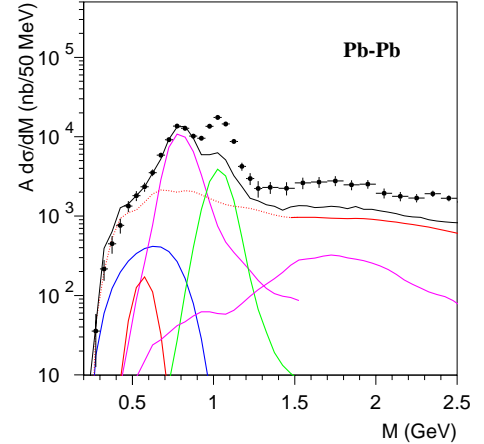
Table 5 collects the ratios (and their statistical uncertainties) between the measured data and the sum of expected sources, for three mass intervals and for the several
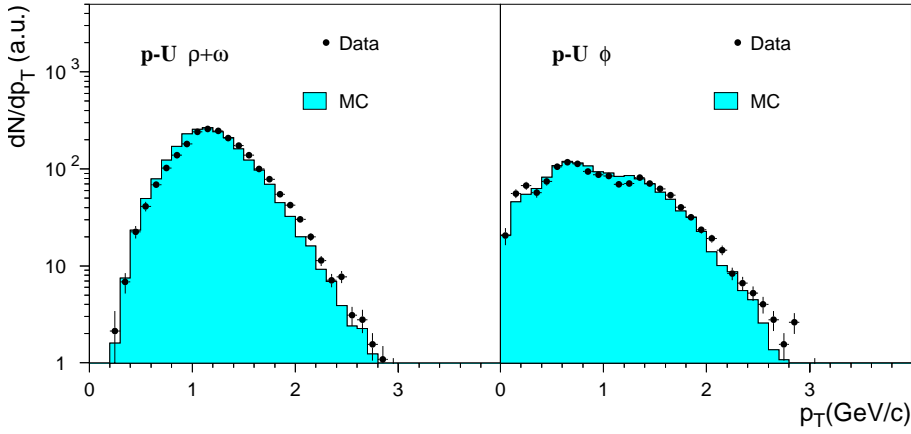
Fig. 9. Transverse momentum distributions measured in p-U collisions, compared with the expected sources, for the $\rho + \omega$ (left) and ϕ (right) mass windows
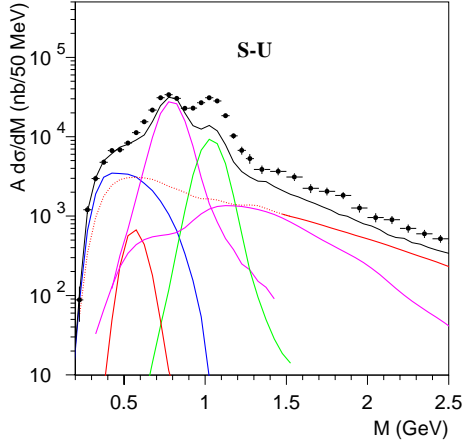
Fig. 10. Dimuon mass distribution measured in S-U collisions, compared to the (extended) cocktail of expected contributions. The curves have the same meaning as in Fig. 5

Table 5. Ratio 'data over sources' in different mass intervals. Only statistical errors are presented

Mass bin (GeV)	p-U	S-Cu	S-U	Pb-Pb
0.40–0.65	1.00 ± 0.02	0.94 ± 0.06	1.18 ± 0.03	–
0.65–0.95	0.99 ± 0.01	1.09 ± 0.03	1.20 ± 0.01	1.08 ± 0.02
0.95–1.20	1.01 ± 0.02	1.58 ± 0.07	2.25 ± 0.04	2.55 ± 0.05

Fig. 11. Dimuon mass distribution measured in Pb-Pb collisions. The low mass region is considerably affected by the stronger m_T cut applied in this data set. The curves have the same meaning as in Fig. 5
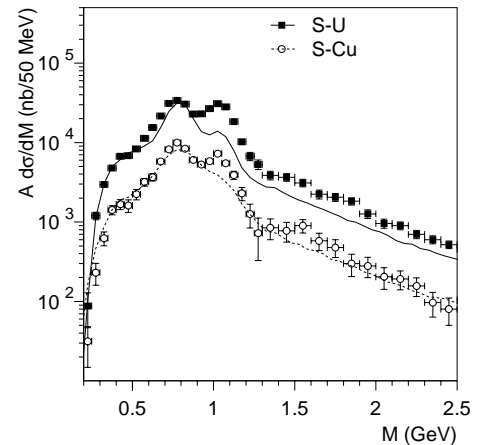

Fig. 12. Dimuon mass spectra measured in S-Cu and S-U collisions, compared, in each case, with the corresponding expected sources

data sets studied in this work. We see that the mass window below the ϕ peak in our nucleus-nucleus data do not exhibit a strong excess relative to our (extended) cocktail of 'expected sources', previously seen to describe reasonably well the p-U spectra.

These results are not necessarily in contradiction with the large excess seen by the CERES experiment since the two detectors probe rather different kinematical regions, specially in what concerns the transverse momentum of the dileptons. Once more we see the need for future data, extending through a broad p_T range, to fully clarify these observations.

In view of the somewhat speculative nature of our conjecture that $q\bar{q}$ annihilations are an important source of high-p_T low mass dileptons, and given the large uncertainty affecting our rough estimation of its mass distribution, we have also compared the measured data to the sum of the 'classical expected sources'. In this case, the S-U data exceeds the 'hadronic cocktail' by a factor 1.75 ± 0.11,
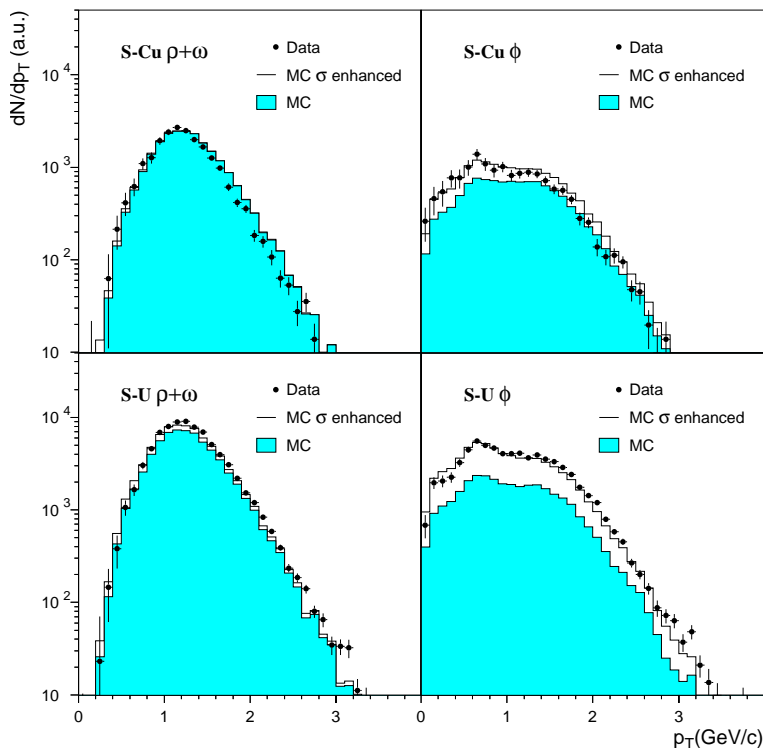
Fig. 13. Transverse momentum distributions measured in S-Cu (top) and S-U (bottom), compared with the expected sources, for the $\rho+\omega$ (left) and ϕ (right) mass windows

in the mass window 0.4–0.65 GeV. The fact that this value is significantly higher than the corresponding value in the p-U data lends further support to the hypothesis that the excess dimuons have a stronger 'A-dependence' than the hadronic sources.

As we did for the p-U analysis, we must check that the event generation was done with p_T distributions that are in reasonable agreement with the available ion data. In Fig. 13 we compare the transverse momentum distributions measured in the $\rho+\omega$ and ϕ mass windows, in S-Cu and S-U collisions, with the expected contributions, simulated by Monte-Carlo. Besides the expected normalisation, shown as a shaded area, we also show a curve obtained by enhancing the production cross-section of the corresponding resonances. We conclude that the model used in our calculations gives a proper representation of the measured p_T distributions.

We have redone the analysis of the S-U and Pb-Pb data with mass dependent p_T distributions, using $T = 220$ MeV for the η, 240 MeV for the ρ and ω, and 260 MeV for the η' and ϕ. For the mass windows below 950 MeV the results change by less than 3 %. In the ϕ peak, the excess decreases by 4 % in S-U and by 12 % in Pb-Pb.

7 Conclusions

In this paper we reported the results of a study of the low mass dimuons produced in p-U and in nucleus-nucleus collisions, as measured by the NA38 and NA50 experiments. This study followed very closely the ideas and methods developed by the CERES collaboration for the correspond-

ing analysis of di-electron production, adapted to the specific conditions of our data.

The comparison of the p-U data to the superposition of the calculated contributions from hadronic decays (including the decays of charmed mesons) reveals a significant excess (~ 30–$40\,\%$) of dimuons in the mass window below the $\rho+\omega$ peak. We have verified that the calculated spectrum cannot be increased in this mass window by reasonable changes in the assumed kinematical distributions of the light mesons. In particular, the kinematical distributions of the ω meson, which significantly contributes to the mass window below 650 MeV through its Dalitz decay, are constrained by the data available in the $\rho+\omega$ peak.

The observation that the 'excess' events have a harder p_T distribution than the muon pairs from η and ω Dalitz decays indicates that they may be due to $q\bar{q}$ annihilations, made visible in our data because of the m_T cut applied by the muon spectrometer. We have shown that this hypothesis is compatible with the analysis of the CERES p-A data. When we add to the standard hadronic cocktail the contribution from low mass $q\bar{q}$ annihilations, naively estimated by extrapolating down in mass the Drell-Yan process, we find a reasonable description of the measured p-U data.

The S-Cu, S-U and Pb-Pb data, measured with the same basic detector, also exhibit a higher dimuon yield than what would be expected on the basis of the standard hadronic cocktail. We have found that the same 'low mass $q\bar{q}$ annihilations' process, scaled with the linear dependence on the product of the projectile and target mass numbers typical of hard processes, is able to roughly reproduce the excess dimuon yield seen in these nucleus-nucleus collisions. We hope that these observations will motivate

sound theoretical work towards a solid calculation of low mass (but high p_T) Drell-Yan production.

References

1. G. Roche et al., Phys. Rev. Lett. **61** (1988) 1069. M.R. Adams et al., Phys. Rev. **D27** (1983) 1977. D. Blockus et al., Nucl. Phys. **B201** (1982) 205. S. Mikamo et al., Phys. Lett. **106B** (1981) 428. J. Ballam et al., Phys. Rev. Lett. **41** (1978) 1207. T. Åkesson et al., Phys. Lett. **B192** (1987) 463.

2. K.J. Anderson et al., Phys. Rev. Lett. **37** (1976) 799. J.G. Branson et al., Phys. Rev. Lett. **38** (1977) 1334. B. Haber et al., Phys. Rev. **D22** (1980) 2107. D.M. Grannan et al., Phys. Rev. **D18** (1978) 3150. H. Kasha et al., Phys. Rev. Lett. **36** (1976) 1007.

3. R. Veenhof, Universiteit van Amsterdam, PhD thesis, 1993. T. Åkesson et al. (HELIOS/1 Coll.), Z. Phys. **C68** (1995) 47.

4. G. Agakichiev et al. (CERES Coll.), Eur. Phys. J. **C4** (1998) 231.

5. G. Agakichiev et al. (CERES Coll.), Eur. Phys. J. **C4** (1998) 249.

6. G. Agakichiev et al. (CERES coll.), Phys. Rev. Lett. **75** (1995) 1272. G. Agakichiev et al. (CERES coll.), Phys. Lett. **B422** (1998) 405.

7. A. Angelis et al. (HELIOS/3 Coll.), CERN-EP/98-82.

8. C. Lourenço et al. (NA38 Coll.), Nucl. Phys. **A 566** (1994) 77c. E. Scomparin et al. (NA50 Coll.), Nucl. Phys. **A 610** (1996) 331c.

9. E. Scomparin et al. (NA50 Coll.), Proceedings of the "Strangeness in Quark Matter 98" Conference, Padova, Italy, July 1998, J. Phys. G: Nucl. Part. Phys. **25** (1999) 235; C. Soave et al. (NA50 Coll.), Proceedings of the "XXIX International Conference on High Energy Physics, CHEP'98", Vancouver, Canada, July 1998.

10. A. de Falco, PhD Thesis, Università di Cagliari, 1997. A. de Falco et al. (NA50 Coll.), Nucl. Phys. **A 638** (1998) 487c.

11. L. Anderson et al. (NA10 Coll.), Nucl. Instrum. Meth. **223** (1984) 26.

12. J.C. Collins and D.E. Soper, Phys. Rev. **D16** (1977) 2219.

13. C. Lourenço, PhD Thesis, Universidade Técnica de Lisboa, 1995.

14. R. Mandry, PhD Thesis, Université Claude Bernard, Lyon, 1993.

15. M.C. Abreu et al. (NA50 Coll.), Phys. Lett. **B410** (1997) 327; Phys. Lett. **B410** (1997) 337.

16. M. Aguilar-Benitez et al. (NA27 Coll.), Z. Phys. **C50** (1991) 405.

17. W. Busza and R. Ledoux, Ann. Rev. Nucl. Part. Sci. **38** (1988) 119.

18. G.J. Gounaris and J.J. Sakurai, Phys. Rev. Lett. **21** (1968) 244.

19. A. Angelis et al. (HELIOS/3 Coll.), Eur. Phys. J. **C5** (1998) 63.

20. N. Kroll and W. Vada, Phys. Rev. **98** (1955) 1355.

21. L.G. Landsberg, Phys. Rep. **128** (1985) 301.

22. J. Bächler et al. (NA35 Coll.), Z. Phys. **C51** (1991) 157; M. Gaździcki and D. Röhrich, Z. Phys. **C65** (1995) 215.

23. R.M. Barnett et al., Phys. Rev. **D54** (1996) 1.

24. M.Kh. Anikina et al., Soviet Journal of Nuclear Physics, Yad. Fiz. **38** (1983) 88; (Dubna Report 1-82-553).

25. T. Sjöstrand, Comp. Phys. Comm. **82** (1994) 74.

26. M. Glück, E. Reya and A. Vogt, Z. Phys. **C53** (1992) 127; M. Glück, E. Reya and A. Vogt, Phys. Lett. **B306** (1993) 391.

27. P. Braun-Munzinger et al., Euro. Phys. J. C **1** (1998) 123.

28. M. Glück, E. Reya and A. Vogt, Z. Phys. **C67** (1995) 433.

29. A.D. Martin, R.G. Roberts and W.J. Stirling, Phys. Rev. **D51** (1995) 4756.